Analysis of Homeostatic Mechanisms in Biochemical Networks

Michael Reed, Janet Best, Martin Golubitsky, Ian Stewart & H. Frederik Nijhout

Volume 79 • Number 11
November 2017

Bulletin of Mathematical Biology

A Journal Devoted to Research at the Junction of Computational, Theoretical, and Experimental Biology
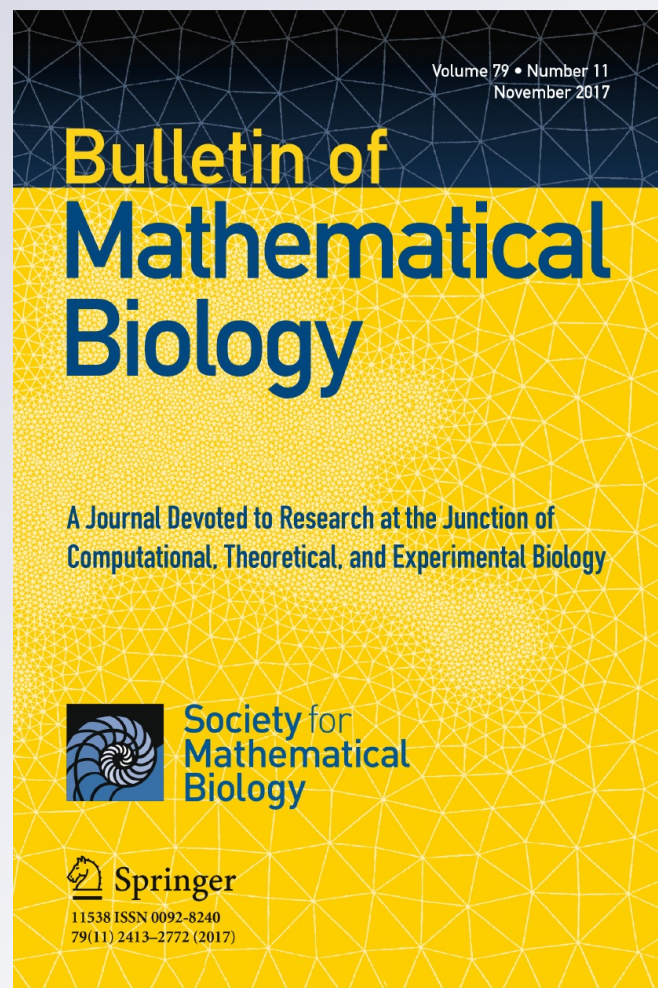
Society for Mathematical Biology

Springer
11538 ISSN 0092-8240
79(11) 2413–2772 (2017)

Springer

Springer

Society for Mathematical Biology

CrossMark

ORIGINAL ARTICLE

Analysis of Homeostatic Mechanisms in Biochemical Networks

Michael Reed[1] · **Janet Best**[2] · **Martin Golubitsky**[2] · **Ian Stewart**[3] · **H. Frederik Nijhout**[4]

Abstract Cell metabolism is an extremely complicated dynamical system that maintains important cellular functions despite large changes in inputs. This "homeostasis" does not mean that the dynamical system is rigid and fixed. Typically, large changes in external variables cause large changes in some internal variables so that, through various regulatory mechanisms, certain other internal variables (concentrations or velocities) remain approximately constant over a finite range of inputs. Outside that range, the mechanisms cease to function and concentrations change rapidly with changes in inputs. In this paper we analyze four different common biochemical homeostatic mechanisms: feedforward excitation, feedback inhibition, kinetic homeostasis, and parallel inhibition. We show that all four mechanisms can occur in a single biological network, using folate and methionine metabolism as an example. Golubitsky and Stewart have proposed a method to find homeostatic nodes in networks. We show that

✉ Michael Reed
   reed@math.duke.edu

   Janet Best
   best.82@osu.edu

   Martin Golubitsky
   golubitsky.4@osu.edu

   Ian Stewart
   I.N.Stewart@warwick.ac.uk

   H. Frederik Nijhout
   hfn@duke.edu

[1]   Department of Mathematics, Duke University, Durham, NC 27708, USA

[2]   Department of Mathematics, The Ohio State University, Columbus, OH 43210, USA

[3]   Mathematics Institute, University of Warwick, Coventry CV47AL, UK

[4]   Department of Biology, Duke University, Durham, NC 27708, USA

their method works for two of these mechanisms but not the other two. We discuss the many interesting mathematical and biological questions that emerge from this analysis, and we explain why understanding homeostatic control is crucial for precision medicine.

1 Introduction

The concept of homeostasis has a long history in physiology going back to the French physiologist Claude Bernard who emphasized the importance of maintaining *"le milieu intérieur"*. The word homeostasis itself was introduced by the American physiologist Walter Bradford Cannon (1926). In studying homeostasis, classical physiologists were mainly concerned with the mechanisms that regulated whole body variables like temperature, plasma sodium and glucose levels, and muscle tone, and kept them within certain narrow limits. Figure 1 shows a recent example: the cerebral blood flow is quite homeostatic as blood pressure varies. Homeostasis also occurs in biochemical systems: Fig. 2 shows the homeostasis of fructose 2,6-biphosphate (an important regulator of glycolysis) in an insect as the hormone corpora cardiaca is varied.

In our own work on cell metabolism, we have found many such mechanisms that buffer certain concentrations against large changes in amino acid inputs and protect cells against genetic polymorphisms that occur in the genes that code for enzymes.
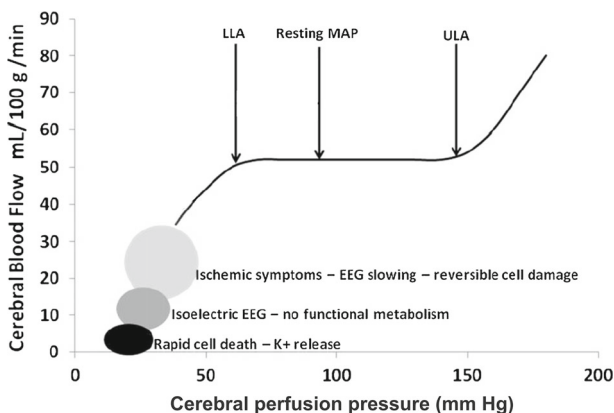
Fig. 1 Homeostasis in cerebral blood perfusion. The *horizontal axis* is cerebral perfusion pressure and the *vertical axis* is cerebral blood flow in humans. Because of numerous homeostatic mechanisms, the cerebral blood flow shows remarkable homeostasis over a wide range of pressures. LLA and ULA indicate the *lower* and *upper* limits of pressures between which the homeostatic mechanisms work well. MAP indicates the mean arterial pressure while resting. Once one leaves the homeostatic region, serious health effects occur. The figure is redrawn from Green and Lee (2012)

Fig. 2 Homeostasis of fructose 2,6-biphosphate. Fructose 2,6-biphosphate is an important regulatory molecule in glycolysis. It, in turn, is regulated in insects (measurements in *Blaptica dubia*) by a hormone fr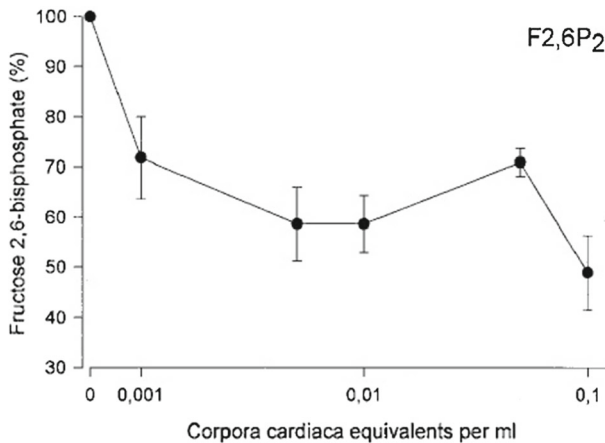om the corpora cardiaca. Fructose 2,6-biphosphate shows homeostasis as the amount of corpora cardiaca hormone is varied. The figure is redrawn from Becker et al. (1996)

We have been continually surprised that even relatively small networks can have many overlapping regulatory mechanisms. This is true in one-carbon metabolism Nijhout et al. (2004), Reed et al. (2008, 2014), and it is true in dopamine and serotonin metabolism in the brain Best et al. (2009, 2010). The study of such mechanisms is central to understanding cell metabolism and also important for designing intervention strategies when the mechanisms do not work, as is the case in many disease states. Indeed, such regulatory mechanisms typically work only when the challenges that the cell faces are within a finite range. Outside that range, the mechanisms become ineffective, and the variables that the mechanisms are supposed to control change rapidly, a phenomenon that Nijhout et al. (2014) call "escape from homeostasis." One can see the escape from homeostasis in both Figs. 1 and 2. Another example, in bone remodeling, can be found in Elliott et al. (2016). Nijhout and Reed (2014) called such graphs "chairs," where one variable shows both homeostasis and escape from homeostasis with respect to another. We note that in Drengstig et al. (2012), two-node input–output motifs are classified, and the three-dimensional surfaces show many chair curves.

Cell metabolism is an extremely complicated dynamical system, and it is important to understand that "homeostasis" does not mean that the dynamical system is rigid and fixed in the face of changes in external variables. Far from it. Typically, large changes in external variables cause large changes in some internal variables so that, through the regulatory mechanisms, certain other internal variables (concentrations or velocities) remain homeostatic. For reasons that we will make clear in the discussion, understanding homeostatic control is crucial for precision medicine.

The work of Nijhout, Best, and Reed on homeostasis Nijhout and Reed (2014), Nijhout et al. (2014, 2015) led Golubitsky and Stewart (2017) to the idea of using singularity theory to identify which nodes in a dynamical systems network could be

Fig. 3 The feedforward
excitation motif. The substrate X
activates the enzyme that
catabolizes Z
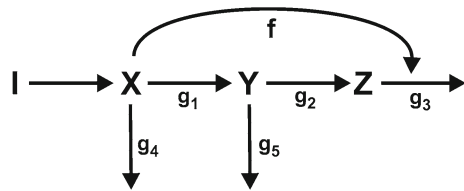
homeostatic with respect to certain input variables. They observed that a typical "chair" curve looks approximately like a function of the form $\mathbb{C}(\lambda) = (\lambda - a)^3 + b(\lambda - a) + c$ where b is small. See, for example, the curves in Fig. 4. Thus, if z is the variable that one hopes is homeostatic and if $z(I)$ is the steady-state value of z as a function of the input to the network, I, then one should search for a value I_0 of I such that both $z'(I_0) = 0$ and $z''(I_0) = 0$. If $z'(I_0) = 0$ but $z''(I_0) \neq 0$, we call I_0 a *GS homeostasis point*. If both $z'(I_0) = 0$ and $z''(I_0) = 0$, but $z'''(I_0) \neq 0$, we call I_0 a *GS chair point*. One can search for GS homeostasis points and GS chair points by using implicit differentiation on the equations describing the conditions for steady states. If one finds a GS chair point at I_0 for a set of parameters, p_o, then singularity theory guarantees that, for p in a small neighborhood of p_o, one can find corresponding curves $z_p(I)$ such that $z_p(I)$ is similar to $z_{p_o}(I)$, but $z'(I_o)$ and $z''(I_0)$ are small with either sign. That is, $z_p(I)$ will show homeostasis even though $z'(I) \neq 0$ and $z''(I) \neq 0$ for any I near I_o.

In this paper, we present mathematical analyses of four common homeostatic mechanisms in cell metabolism: feedforward excitation, feedback inhibition, kinetic homeostasis, and parallel inhibition (Sects. 2–5). We show that feedforward excitation and kinetic homeostasis can arise from GS chair points, but feedback inhibition and parallel inhibition cannot. In Sect. 6, we show that several mechanisms can occur simultaneously in a small network resulting in a chair with three steps. In Sect. 7, we examine a real metabolic network, folate and methionine metabolism, and show that all four motifs occur there. In the discussion (Sect. 8), we point out many interesting biological and mathematical questions suggested by this work.

2 The Feedforward Excitation Motif

Feedforward excitation occurs in a biochemical network when a substrate activates the enzyme that removes a product, as depicted in Fig. 3. We will see a biological example of feedforward excitation in Sect. 7. In all of our motif diagrams, X, Y, and Z are the names of chemical substrates, and we denote their concentrations (in units of micromolar, for example) by lower case x, y, and z. Each straight arrow represents a flux (in micromolar/hour, for example) coming into or going away from a substrate. The differential equations for each substrate simply say that the rate of change of the concentration is the sum of the arrows going toward substrate minus the arrows going away. Curved lines (see Figs. 3, 5, 9, 11) indicate that a substrate is activating an enzyme (pointed) or inhibiting an enzyme (barred).

To gain intuition, we start by considering the simple case where each g_i has linear mass-action kinetics, $g_i(x) = c_i x$, and the feedforward excitation (f) has simple product form. Then the differential equations are:

$$\dot{x} = I - c_4 x - c_1 x$$
$$\dot{y} = c_1 x - c_2 y - c_5 y$$
$$\dot{z} = c_2 y - f(x)z. \tag{1}$$

where the assumption $f' > 0$ would correspond to feedforward activation because as x gets larger the rate of removal of z increases. We always suppose that $f > 0$ if $x > 0$. First suppose f is a positive constant (no feedforward activation). Then, it is easy to check that at equilibrium all three concentrations, $x(I)$, $y(I)$, and $z(I)$, will grow linearly in I. However, if $f' > 0$, then $z(I)$ could be homeostatic, because as I goes up, the increased synthesis of Z could be balanced by increased catabolism. We will see that this is true for an appropriate choice of f and that the system has a GS chair. The equilibria can easily be calculated explicitly:

$$x(I) = \frac{1}{c_1 + c_4} I; \quad y(I) = \frac{c_1}{(c_2 + c_5)(c_1 + c_4)} I;$$
$$z(I) = \frac{c_1 c_2}{(c_1 + c_4)(c_2 + c_5)} \frac{I}{f\left(\frac{I}{c_1 + c_4}\right)}.$$

To simplify the calculation, let $\hat{I} = I/(c_1 + c_4)$ and $\hat{c} = c_1 c_2 / (c_2 + c_5)$. Then,

$$z(\hat{I}) = \hat{c} \frac{\hat{I}}{f(\hat{I})}$$

GS homeostasis occurs when $z' = 0$, and GS chairs occur when $z'' = z' = 0$, where $'$ indicates differentiation with respect to $\hat{I}$. Since GS points are independent of $\hat{c}$, we may assume $\hat{c} = 1$. Since

$$z'(\hat{I}) = \frac{1}{f(\hat{I})} - \frac{\hat{I} f'(\hat{I})}{f(\hat{I})^2}, \tag{2}$$

a GS homeostasis point occurs at $\hat{I}$ when

$$f'(\hat{I}) = \frac{f(\hat{I})}{\hat{I}}. \tag{3}$$
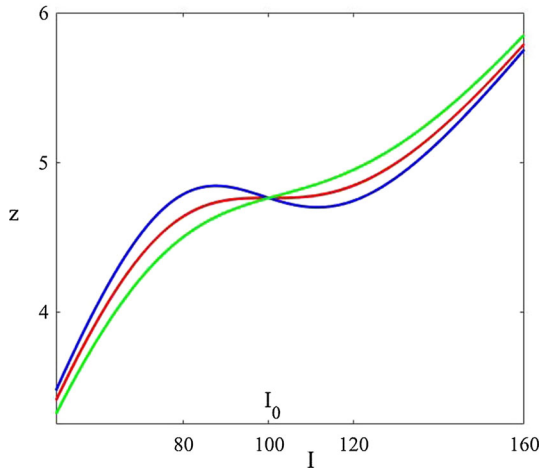
Differentiating (2) and using (3), we find

$$z'' = -2\frac{f'}{f^2} + 2\frac{\hat{I}(f')^2}{f^3} - \frac{\hat{I} f''}{f^2} = -\frac{\hat{I} f''}{f^2}$$

so a GS chair occurs at a point $\hat{I}$ where

$$f'(\hat{I}) = \frac{f}{\hat{I}} \quad \text{and} \quad f''(\hat{I}) = 0.$$

Fig. 4 Simulations of the feedforward excitation motif. Here $c_1 = c_2 = c_4 = 1$, $c_5 = 6$, $f(x) = 1 + 1/\left[1 + exp\left(\frac{50-x}{\sigma}\right)\right]$. The GS chair point occurs at $I_0 = 100$. For the *red curve*, $\sigma = 8.33$, for the *blue curve* $\sigma = 7$, and for the *green curve* $\sigma = 10$ (Color figure online)

Example Consider the following choice for f:

$$f(x) = 1 + \frac{1}{1 + g(x)} \qquad \text{where} \qquad g(x) = e^{\frac{50-x}{\sigma}}.$$

Recall that along the curve of equilibria $x = \hat{I}$. Note that $g' = -\frac{1}{\sigma}g$ and $g'' = \frac{1}{\sigma^2}g$. We can calculate the derivatives of f in terms of g. In particular, $f'' = 0$ implies $g(\hat{I}) = 1$, which in turn implies $\hat{I} = 50$. It follows that $I = (c_1 + c_4)\hat{I} = 100$. Next, use $g(\hat{I}) = 1$ to compute

$$f' = -\frac{g'}{(1 + g)^2} = \frac{1}{\sigma}\frac{g}{(1 + g)^2} = \frac{1}{4\sigma}$$

It follows that

$$\frac{3}{2} = f(\hat{I}) = \hat{I}f'(\hat{I}) = \frac{50}{4\sigma}.$$

Therefore, $\sigma = \frac{25}{3}$. The fact that a GS chair occurs at $\sigma \approx 8.33$ and $I = 100$ is confirmed by numerical calculations; see the red curve in Fig. 4.

For nearby choices of parameters, $\sigma = 7$ or $\sigma = 10$, the curve $z(I)$ shows homeostasis but can be always increasing (green) or have a decreasing portion (blue). In all three cases, the curves show escape from homeostasis when I is large or small because in the corresponding ranges of $x(I)$, f is close to constant and, as we explained in the beginning, when f is constant the equilibria scale linearly in I. This escape from homeostasis is what one sees in real biological examples because the homeostatic mechanisms work over only a finite range of input values. See Figs. 1 and 2 and Nijhout et al. (2014).

We now show that these calculations can be done quite generally. The differential equations are:

$$\dot{x} = I - g_1(x) - g_4(x)$$
$$\dot{y} = g_1(x) - g_2(y) - g_5(y)$$
$$\dot{z} = g_2(y) - h(x, z),$$
(4)

and feedforward excitation is represented by the following conditions on h:

$$\frac{\partial h}{\partial x} > 0 \quad \text{and} \quad \frac{\partial h}{\partial z} > 0.$$
(5)

Note that (1) is a special case of (4). It is convenient to define a specific space of kinetic functions.

Definition 1 Let $\mathbb{G}$ be the set of real-valued functions on $[0, \infty)$ such that each $g \in \mathbb{G}$ satisfies:

(i) g is twice continuously differentiable, and $g'(x) > 0$ for all x.
(ii) $g(0) = 0$.
(iii) $g(x) \rightarrow \infty$ as $x \rightarrow \infty$.

We note that $\mathbb{G}$ is a group under composition.

Theorem 2 *Suppose $g_i \in \mathbb{G}$ for each i. Suppose that h is twice continuously differentiable, $h(x, \cdot) \in \mathbb{G}$ for each $x > 0$, and h satisfies* (5). *Then there is a unique stable equilibrium $(x(I), y(I), z(I))$ for each I. GS homeostasis occurs at I_0 if and only if*

$$h_x(x_0, z_0) = \frac{g_1' g_2'}{g_2' + g_5'}$$
(6)

where $(x_0, y_0, z_0) = (x(I_0), y(I_0), z(I_0))$ and the g_i' are evaluated at x_0, y_0 or z_0 as appropriate.

A GS chair occurs at I_0 if and only if (6) *and*

$$h_{xx}(x_0, z_0) = \frac{1}{g_2' + g_5'} \left(g_1'' g_2' + (g_1')^2 \frac{g_2'' g_5' - g_2' g_5''}{(g_2' + g_5')^2} \right).$$
(7)

Proof The equations for equilibria in (4) are:

$$I - g_4(x(I)) - g_1(x(I)) = 0$$
$$g_1(x(I)) - g_2(y(I)) - g_5(y(I)) = 0$$
$$g_2(y(I)) - h(x(I), z(I)) = 0$$
(8)

We first show that (8) has a unique solution $(x(I), y(I), z(I))$ for each I, and the corresponding equilibrium for (4) is linearly stable. Since $g_1 + g_4$ is an unbounded

increasing function that vanishes at the origin, there is a unique solution $x(I) > 0$ to the first equation, $g_1(x) + g_4(x) = I$. Similarly, since $g_2 + g_5$ is an unbounded increasing function that vanishes at the origin, there is a unique solution $y(I) > 0$ to the second equation, $g_2(y) + g_5(y) = g_1(x(I))$. Finally, for each I, there is a unique solution $z(I) > 0$ to the third equation, $h(x(I), z) = g_2(y(I))$, since by (5), $h(x, \cdot)$ is unbounded, strictly monotone increasing, and vanishes at the origin. Finally, at an equilibrium, the Jacobian of (8) is

$$
J = \begin{pmatrix}
-(g_1' + g_4') & 0 & 0 \\
g_1' & -(g_2' + g_5') & 0 \\
-h_x & g_2' & -h_z'
\end{pmatrix}
$$

all of whose eigenvalues are negative, so the equilibrium is asymptotically stable.

Next we discuss GS points. Differentiate (8) with respect to I obtaining

$$
\begin{aligned}
(g_1' + g_4')x' &= 1 \\
g_1'x' - (g_2' + g_5')y' &= 0 \\
g_2'y' - h_x x' - h_z z' &= 0
\end{aligned}
\tag{9}
$$

Solve the first equation for x' and the second equation for $\frac{y'}{x'}$ obtaining

$$
x' = \frac{1}{g_1' + g_4'} \quad \text{and} \quad \frac{y'}{x'} = \frac{g_1'}{g_2' + g_5'}
\tag{10}
$$

The third equation then implies that $z' = 0$ if and only if (6) is satisfied.

Next differentiate (9) with respect to I and evaluate at $z' = z'' = 0$ to obtain

$$
\begin{aligned}
(g_1' + g_4')x'' + (g_1'' + g_4'')(x')^2 &= 0 \\
g_1'x'' + g_1''(x')^2 - (g_2' + g_5')y'' - (g_2'' + g_5'')(y')^2 &= 0 \\
g_2'y'' + g_2''(y')^2 - h_{xx}(x')^2 - h_x x'' &= 0
\end{aligned}
$$

which we can rewrite as

$$
\begin{aligned}
\frac{x''}{(x')^2} &= -\frac{g_1'' + g_4''}{g_1' + g_4'} \\
(g_2' + g_5')\frac{y''}{(x')^2} &= g_1'\frac{x''}{(x')^2} + g_1'' - (g_2'' + g_5'')\left(\frac{y'}{x'}\right)^2 \\
h_{xx} &= g_2'\frac{y''}{(x')^2} + g_2''\left(\frac{y'}{x'}\right)^2 - h_x\frac{x''}{(x')^2}
\end{aligned}
\tag{11}
$$

Next use (10) and the first equation in (11) to solve the second equation in (11) for $\frac{y''}{(x')^2}$ obtaining

Fig. 5 The feedback inhibition motif. The substrate Z inhibits the enzyme that catalyzes the conversion of X to Y
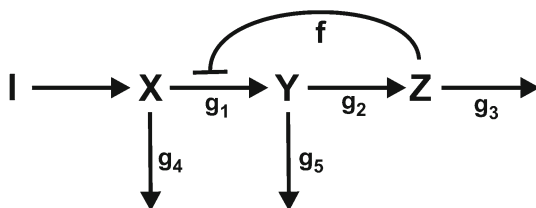
$$\frac{y''}{(x')^2} = \frac{1}{g_2' + g_5'} \left(g_1'' - g_1' \frac{g_1'' + g_4''}{g_1' + g_4'} - (g_1')^2 \frac{g_2'' + g_5''}{(g_2' + g_5')^2} \right)$$

Substitute the formulas for $\frac{x''}{(x')^2}$, $\frac{y''}{(x')^2}$, $\frac{y'}{x'}$ in the third equation in (11) and simplify to yield (7).   □

This theorem can be used to construct examples of homeostasis created by feedforward excitation as we did in the example above. The hypothesis that $g_i(x) \to \infty$ for each i excludes Michaelis–Menten kinetics. However, that hypothesis was used only to show that an equilibrium exists for each $0 \leq I < \infty$. If the g_i satisfy Michaelis–Menten kinetics (or other saturating kinetics), then there will be no equilibrium for I large enough because mass cannot leave the system as fast as it is coming in. In that case, there will be a finite interval, $[0, I_1)$, on which the theorem holds true, and the proof is the same. So the issue with Michaelis–Menten kinetics is only the existence of equilibria, not the effect of feedforward excitation.

3 The Feedback Inhibition Motif

Feedback inhibition is probably one of the simplest and best known homeostatic mechanisms in biochemistry. In its simplest form, feedback inhibition means that the product of a biochemical chain inhibits one or more of the enzymes involved in its own synthesis. Thus if the concentration of the end product goes up, synthesis is slowed, and if the concentration goes down, the inhibition is partially withdrawn and the synthesis goes faster. See Fig. 5.

Examples of feedback inhibition abound, and we mention three. Phosphofructokinase is the third enzyme in glycolysis and is strongly inhibited by the end product ATP Hall (2017). S-adenosylmethionine (SAM) is the universal methyl group donor in cells. There are more than 150 different reactions, each catalyzed by a different enzyme, in which SAM gives up a methyl group and is transformed into S-adenosylhomocysteine (SAH). Almost all of these enzymes are inhibited by SAH Clarke and Banfield (2001), Reed et al. (2014). Third, the enzyme tyrosine hydroxylase catalyzes the key step in the synthesis of dopamine (DA) in neuronal terminals, and it is inhibited by cytosolic DA. Cytosolic DA is packaged into vesicles, and some are released when an action potential arrives. In the extracellular space, DA binds to auto receptors on the terminals that inhibit tyrosine hydroxylase and the release of vesicles. Thus both the cytosolic and the extracellular concentrations of DA are regulated by feedback inhibition Benoit-Marand et al. (2001), Best et al. (2009).

Fig. 6 Homeostasis and escape in the product inhibition motif. In this simulation, $g_i(x) = x$ for all i and $f(z) = 1 + 200/(1 + exp(z - 50)/0.5)$. At equilibrium, $z(I)$ grows linearly for small I and large I and in between shows a homeostatic region where $z'(I) > 0$, but $z(I)$ hardly changes at all
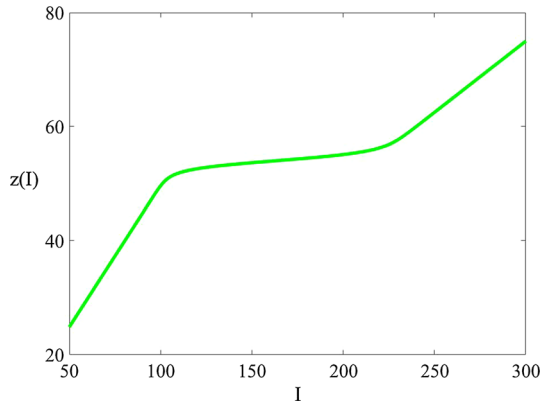
For simplicity and to develop intuition, we first suppose that each of the kinetics, g_i for $i \geq 2$, is linear mass-action, but that $g_1(x)$ is multiplied by a function f that depends on z. The corresponding differential equations are:

$$\dot{x} = I - c_4 x - f(z)c_1 x$$
$$\dot{y} = f(z)c_1 x - c_2 y - c_5 y$$
$$\dot{z} = c_2 y - c_3 z. \tag{12}$$

Product inhibition would be expressed by the hypothesis $f' < 0$. Suppose, instead, that f is a positive constant. Then it is easy to see that for each I, there is a unique steady state $(x(I), y(I), z(I))$, and that the three functions $x(I), y(I), z(I)$ are each linearly increasing in I. However, if $f' < 0$, then, as z goes up with I, f will inhibit the synthesis of z, which will moderate the increase. Figure 6 shows the result for particular choices of the constants c_i and the function f. The variable $z(I)$ shows very strong homeostasis in the middle range of I but shows the escape from homeostasis for low I or high I because f is almost constant for low and high z. Of course we have chosen the function f in order to make this point. Rather than the simple product form, $f(z)c_1 x$, in this example, in general the kinetics of the reaction from X to Y will be given by $h(x, z)$, where $\frac{\partial h}{\partial x} > 0$ (more substrate, faster reaction) and $\frac{\partial h}{\partial z} < 0$ (higher Z, more inhibition of the reaction). See Eq. (13).

Though the feedback inhibition motif can create a strongly homeostatic region, it cannot have a GS singularity. We will prove this by showing, under quite general hypotheses, that $\frac{\partial z}{\partial I} > 0$ for all I. For brevity, we omit the proof of existence of the equilibrium for all I and just give the local result. The differential equations are:

$$\dot{x} = I - g_4(x) - h(x, z)$$
$$\dot{y} = h(x, z) - g_2(y) - g_5(y)$$
$$\dot{z} = g_2(y) - g_3(z). \tag{13}$$

Theorem 3 *Suppose that $g_i \in \mathbb{G}$ for all i. Suppose that $h(x, z)$ is continuously differentiable in the positive orthant, $h > 0$, $\frac{\partial h}{\partial x} > 0$, and $\frac{\partial h}{\partial z} < 0$. Suppose (13) has*

an equilibrium in the positive orthant at I_0. Then the equilibrium extends uniquely to equilibria $(x(I), y(I), z(I))$, where the solution functions are smooth, and $\frac{dz}{dI} > 0$ for all I at and near I_0.

Proof Replacing the second equation in (13) by the sum of the first two equations shows that equilibria of (13) satisfy:

$$g_4(x) + h(x, z) = I$$
$$g_4(x) + g_2(y) + g_5(y) = I$$
$$g_2(y) - g_3(z) = 0. \tag{14}$$

Let $E_0 = (x_0, y_0, z_0)$ be a solution to (14) at I_0. The Jacobian of this system at E_0 is

$$J = \begin{pmatrix} g_4' + h_x & 0 & h_z \\ g_4' & g_2' + g_5' & 0 \\ 0 & g_2' & -g_3' \end{pmatrix}$$

whose determinant $-(g_4' + h_x)(g_2' + g_5')g_3' + h_z g_2' g_4'$ is negative by the assumptions on the g_is and h. It follows from the implicit function theorem that solutions extend uniquely to $(x(I), y(I), z(I))$ where $(x(I_0), y(I_0), z(I_0)) = (x_0, y_0, z_0)$. Differentiating (14) with respect to I yields

$$J \begin{pmatrix} x' \\ y' \\ z' \end{pmatrix} = \begin{pmatrix} 1 \\ 1 \\ 0 \end{pmatrix}$$

We use Cramer's rule to solve for $z'(I)$, namely

$$z' = \det(J) / \det \begin{pmatrix} g_4' + h_x & 0 & 1 \\ g_4' & g_2' + g_5' & 1 \\ 0 & g_2' & 0 \end{pmatrix} = \frac{-(g_4' + h_x)(g_2' + g_5')g_3' + h_z g_2' g_4'}{-g_2' h_x}$$

Since $\frac{\partial h}{\partial x} > 0$ and $\frac{\partial h}{\partial z} < 0$, we see that $z'(I) > 0$ as claimed. □

The actual kinetic formulas for inhibitory functions like $h(x, z)$ have been studied extensively Segel (1975), Cornish-Bowden (2012) and depend on the details of the chemical binding of the substrate Z to one or more sites on the enzyme. Thus, the actual kinetic formulas depend on the particular enzyme under consideration. The size of the homeostatic interval and the flatness of the graph depend, of course, on the properties of h.

4 The Kinetic Motif

We now consider the possibility that Z might show homeostasis with respect to the input I because the homeostasis is built into the kinetics between Y and Z. See Fig. 7.

Fig. 7 The kinetic motif. Homeostasis is built into the kinetics from Y to Z
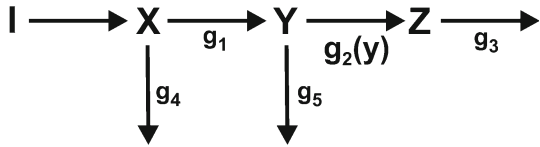
Suppose that $g_2(y)$ has a functional form like one of the curves in Fig. 4. For simplicity, we assume g_1, g_3, g_4, and g_5 have linear mass-action kinetics. Then, the equilibrium equations associated with this system are:

$$(c_1 + c_4)x = I$$
$$g_2(y) + c_5 y = c_1 x$$
$$c_3 z = g_2(y) \tag{15}$$

It follows immediately that x scales linearly in I and that $z(I) = \frac{1}{c_3} g_2(y(I))$, so the shape of $z(I)$ is a rescaling of the shape of $g_2(y(I))$, which is why we call this the kinetic motif.

Consider the general case:

$$\dot{x} = I - g_1(x) - g_4(x)$$
$$\dot{y} = g_1(x) - g_5(y) - g_2(y)$$
$$\dot{z} = g_2(y) - g_3(z) \tag{16}$$

where g_1, g_3, g_4, and g_5 are in $\mathbb{G}$, but $g_2(y)$ can have a more general shape (for example, a negative derivative over certain intervals).

Theorem 4 *Suppose that $g_1, g_3, g_4, g_5 \in \mathbb{G}$, that g_2 is twice continuously differentiable on $\mathbb{R}$ and that $0 < \alpha \le g_5'(y) + g_2'(y)$ for some α. Then, the system (16) has a unique, stable equilibrium for each $I \ge 0$. Furthermore, z has a GS homeostasis point at I_0 if and only if $g_2'(y_0) = 0$ and z has a GS chair point at I_0 if and only if $g_2'(y_0) = g_2''(y_0) = 0$, where $y_0 = y(I_0)$.*

Proof Suppose $I \ge 0$. Since $g_1 + g_4 \in \mathbb{G}$, the first equilibrium equation, $g_1(x) - g_4(x) = I$, can be solved uniquely for $x(I)$ and $x'(I) > 0$. Similarly, since $g_5'(y) + g_2'(y) \ge \alpha$, the second equilibrium equation has a unique solution and $y'(I) > 0$. Since $g_3 \in \mathbb{G}$, the third equilibrium equation can be solved uniquely for $z(I)$. By writing down the Jacobian, it is easy to check that the equilibria are stable. Differentiating $g_2(y(I)) = g_3(z(I))$ with respect to I yields

$$g_2'(y_0)y'(I_0) = g_3'(z_0)z'(I_0).$$

Thus since $y'(I_0) \ne 0$ and $g_3'(z_0) \ne 0$, we see that $z'(I_0) = 0$ if and only if $g_2'(y_0) = 0$. Differentiating again gives

$$g_2''(y_0)(y'(I_0))^2 + g_2'(y_0)y''(I_0) = g_3''(z_0)(z'(I_0))^2 + g_3'(z_0)z'''(I_0) = 0$$

Hence, $z'(I_0) = z''(I_0) = 0$ if and only if $g_2'(y_0) = g_2''(y_0) = 0$. $\qquad \square$

This raises the natural question whether the kinetics of enzymes can have complicated forms like the curves in Fig. 4. We will briefly explain why the answer is "yes." In what follows, Y will be denoted by S and its concentration by $[S]$ and $g_2(y)$ is replaced by $V([S])$ to connect with traditional biochemical notation. S is called the substrate of the reaction and $V([S])$ is called the velocity of the reaction because it is that rate at which the product of the reaction is formed as a function of the concentration of substrate. Panel A of Fig. 8 shows the reaction diagram for "simple" enzyme kinetics that yields the Michaelis–Menten formula Michaelis and Menten (1915) for the rate of product formation, V. The straightforward derivations of all the formulas in Fig. 8 make use of the equilibrium assumption that the reversible reactions in the diagrams are fast compared to rates of product formation Segel (1975). Note that Michaelis–Menten kinetics has a kind of homeostasis since the velocity curve, $V([S])$, becomes flat for large values of $[S]$ though it does not have a homeostasis point or a chair point. The reason is simple. There is only a finite amount of enzyme, so the reaction cannot make product faster than $k_2 E_o$, where E_o is the total amount of enzyme present.

In the 1930s, Haldane introduced the concept of substrate inhibition in which the substrate of the reaction itself inhibits the enzyme that catalyzes the reaction Haldane (1930). There are many different ways in which this can happen, but a simple way is if two molecules of the substrate can bind to the enzyme as shown in Panel B of Fig. 8, and the rate of formation of the product is lower when two substrate molecules are bound than if one is bound (i.e. $k_4 < k_2$). In this case, the velocity curve will first rise to a maximum and then descend to $k_4 E_o$ as $[S]$ gets larger and larger. It is estimated that about 20% of enzymes show substrate inhibition Chaplin and Burke (1990). We have shown that substrate inhibition often occurs for biologically significant regulatory reasons Reed et al. (2010). For example, it occurs in tyrosine hydroxylase and tryptophan hydroxylase (the rate-limiting enzymes for the synthesis of dopamine and serotonin) and in phosphofructokinase in glycolysis. And, as we will see in Sect. 7, substrate inhibition occurs in the folate cycle. In case of substrate inhibition, the kinetic motif would have GS homeostasis point but not a GS chair.

If an enzyme has multiple binding sites for a substrate, then much more complicated velocity curves can occur. Many such biological examples are given in Segel (1975, 1980, 1984), Storey (2004) where kinetic formulas are derived. We give a simple example in Panel C of Fig. 8 in which the velocity curve has the classic chair shape if $k_6 > k_2 > k_4$, and the other constants are chosen appropriately. In such a case, the kinetic motif has a GS chair point. We remark that once a section of a gene for an enzyme codes for a binding site for S, the section can be duplicated to create an enzyme with many binding sites, and it is not surprising that evolution has created such enzymes in order to create homeostatic regions via the kinetic motif.

5 The Parallel Inhibition Motif

In the motif shown in Fig. 9, I_1 is a fixed input, and we consider how the equilibrium value of z changes as a function of I. As I rises, z will start to rise inhibiting, via f_1, the synthesis of x. As x declines, the inhibition of the catabolism of z is withdrawn. Thus z is removed faster, which will tend to keep its steady-state concentration relatively

A

$$E + S \underset{k_{-1}}{\overset{k_1}{\rightleftharpoons}} E{\cdot}S \xrightarrow{k_2} E + P$$

$$V = \frac{k_2 E_0 [S]}{K_1^{-1} + [S]}$$

B

$$E + S \underset{k_{-1}}{\overset{k_1}{\rightleftharpoons}} E{\cdot}S \xrightarrow{k_2} E + P$$

$$S{\cdot}E{\cdot}S \xrightarrow{k_4} E + S + P$$

$$V = \frac{k_2 E_0 [S] + k_4 E_o K_3 [S]^2}{K_1^{-1} + [S] + K_3 [S]^2}$$

C

$$E + S \underset{k_{-1}}{\overset{k_1}{\rightleftharpoons}} E{\cdot}S \xrightarrow{k_2} E + P$$

$$S{\cdot}E{\cdot}S \xrightarrow{k_4} E + S + P$$

$$S{\cdot}E{\cdot}S \xrightarrow{k_6} E + 2S + P$$

$$V = \frac{k_2 E_0 [S] + k_4 E_o K_3 [S]^2 + k_6 E_0 K_3 K_5 [S]^3}{K_1^{-1} + [S] + K_3 [S]^2 + K_3 K_5 [S]^3}$$
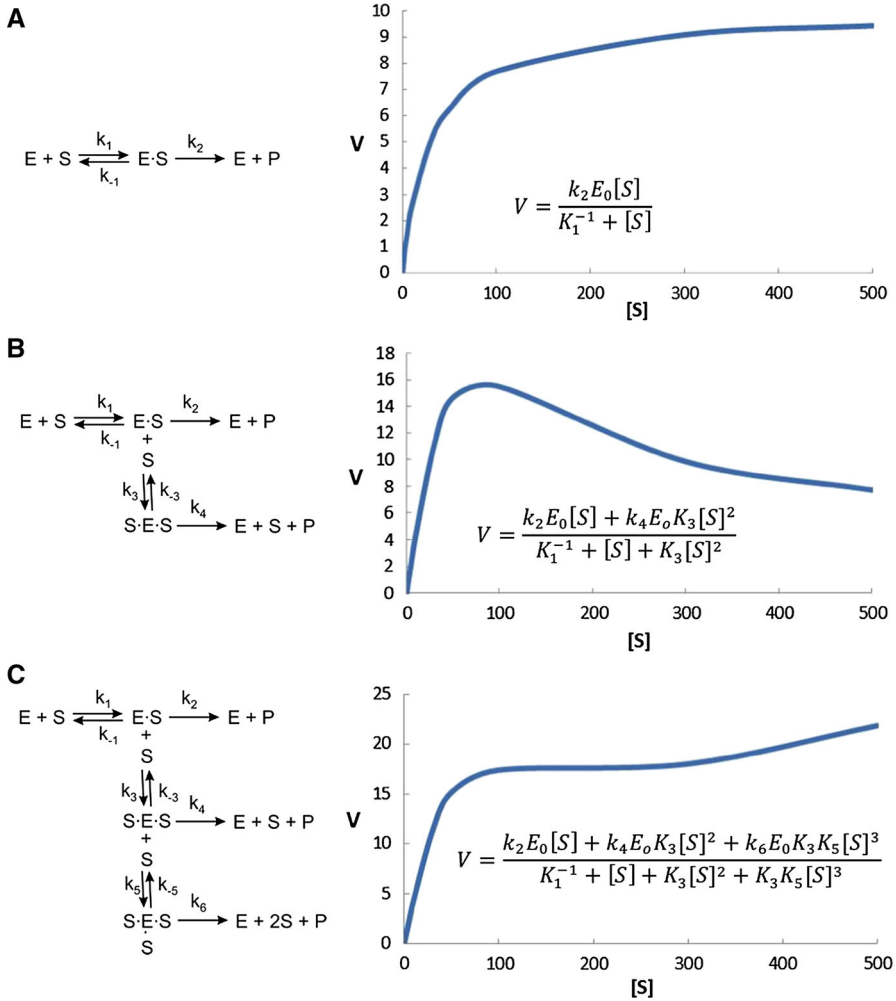

Fig. 8 Multiple binding sites and kinetic formulas. In **a**, we show the simplest reaction diagram for enzyme kinetics that leads to the Michaelis–Menten formula for the velocity, V, in terms of the substrate concentration, $[S]$. The parameters are: $K_1^{-1} = k_{-1}/k_1 = 30$, $k_2 = 1$, $E_0 = 10$. **b** Shows a simple reaction diagram that leads to substrate inhibition if $k_4 < k_2$ and the corresponding velocity curve. The parameters are: $K_1^{-1} = 450$, $k_2 = 2$, $K_3 = k_3/k_{-3} = 0.1$, $k_4 = 0.04$, $E_0 = 100$. **c** Shows an example of enzyme kinetics when there are three binding sites and the corresponding velocity curve. The parameters are: $K_1^{-1} = 450$, $k_2 = 2$, $K_3 = k_3/k_{-3} = 0.1$, $k_4 = 0.04$, $K_5 = k_5/k_{-5} = 0.00003$, $k_6 = 10$, $E_0 = 100$

constant over the ranges in which f_1 and f_2 provide increasing inhibition. We will see this motif in the biological network considered in Sect. 7.

In a simple case, corresponding to Fig. 9, the catabolism of Z would be given by $f_2(x)g_4(z)$. Instead, we immediately consider the general case:

$$\dot{x} = g_1(I_1) f_1(z) - g_3(x)$$
$$\dot{z} = g_2(I) - g_5(z) - h(x, z).$$

Fig. 9 The parallel inhibition motif. The substrate Z inhibits the synthesis of X, and X inhibits an enzyme that catabolizes Z
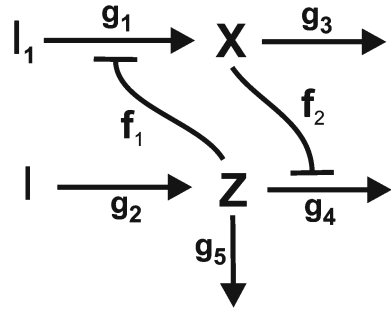
The parallel inhibition hypotheses corresponds to the conditions:

$$\frac{\partial f_1}{\partial z} < 0, \qquad \frac{\partial h}{\partial x} < 0. \qquad (17)$$

Theorem 5 *Suppose that $g_2, g_3, g_4, g_5 \in \mathbb{G}$, that f_1 is positive and continuously differentiable for $z \geq 0$, that h is continuously differentiable in the positive orthant, that $h(x, \cdot) \in \mathbb{G}$ for all $x > 0$, and that (17) holds. Then, for each I, there is a unique stable equilibrium, $(x(I), z(I))$, and $x'(I) < 0$ and $z'(I) > 0$. Thus, z cannot have a GS homeostasis point nor a GS chair point.*

Proof The constant $g_1(I_1)$ does not affect the proof so, for simplicity assume it equals 1. Solving the first equilibrium equation for $x(I)$ in terms of $z(I)$ and substituting in the second equilibrium equation yield:

$$g_2(I) = g_5(z) + h(g_3^{-1}(f_1(z)), z) \equiv F(z). \qquad (18)$$

Differentiating with respect to z,

$$F'(z) = g_5'(z) + \left(\frac{\partial h}{\partial x}\right)(g_3^{-1})' f_1' + \frac{\partial h}{\partial z}.$$

From the parallel inhibition hypotheses (17) and the hypothesis that $h(x, \cdot) \in \mathbb{G}$, it follows that $F'(z) \geq g_5'(z)$ for all $z \geq 0$. Since $F(0) = 0$, Eq. (18) has a unique solution $z(I)$ for each $I \geq 0$ and since g_3 can be inverted the first equilibrium equation yields a unique $x(I)$. It is easy to check that $(x(I), z(I))$ is stable.

Differentiating $F(z(I))$ with respect to I gives:

$$g_2'(I) = \left[g_5'(z) + \frac{\partial h}{\partial x}(g_3^{-1})' f_1' + \frac{\partial h}{\partial z} \right] z'(I),$$

so by the parallel inhibition hypotheses (17), we see that $z'(I) > 0$ and the statements about GS homeostasis points and chair points follow. □

Although the parallel inhibition motif cannot have a GS homeostasis point or a GS chair, nevertheless Z can have a large region of homeostasis as Fig. 10 shows.

Fig. 10 Homeostasis caused by the parallel inhibition motif. In the *middle* region, as I rises, $f_1(x(I))$ inhibits the synthesis of X more and more, so $x(I)$ falls. When $x(I)$ descends to approximately 50 μM, the inhibition of the catabolism of Z by X is withdrawn, $f_2[x(I)]$, and this increased catabolism of Z compensates for the increased synthesis of Z as I rises. f_1 has the form $f_1(z) = 1 + 1/(1 + exp(z - 50)/0.5)$ and f_2 has the form $f_2(x) = 4(1 + 1/[1 + exp(x - 50)])$ $I_1 = 50$ and $g_i(\beta) = \beta$ for each i (Color figure online)
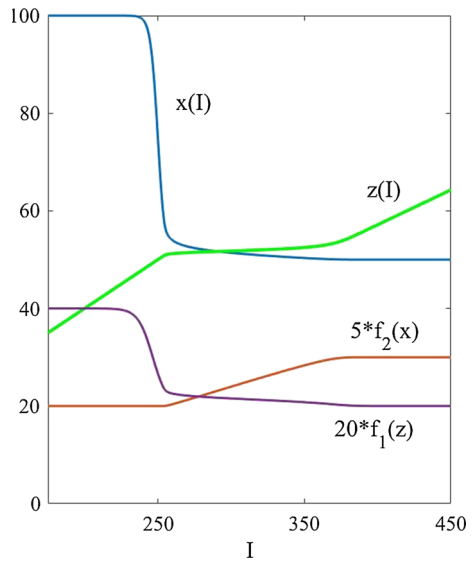
We will describe why $Z(I)$ shows homeostasis between $I = 260$ to $I = 360$ in Fig. 10. Below $I = 240$, both $f_1(z(I))$ and $f_2(x(I))$ are constant so $z(I)$ rises linearly as expected. Once $z(I)$ approaches 50, $f_1(z(I))$ begins to decrease inhibiting the synthesis of X, and so the concentration $x(I)$ decreases rapidly. However, the inhibition of the catabolism of Z does not begin to be withdrawn until $x(I)$ approaches 50. Then every increase in I stimulates lower $x(I)$ which in turn removes inhibition and increases the catabolism of Z, thus keeping Z to a very small rate of increase (the homeostatic plateau). Notice that since $z(I)$ increases very slowly, $x(I)$ decreases slowly in the plateau region. When $x(I)$ and $z(I)$ get far enough away from 50 (for I near 360), then the two inhibitory functions become constant and $z(I)$ begins to rise linearly at a much faster rate. When I is low, $f_1(z(I))$ and $f_2(x(I))$ are constant in I and thus the two pathways have constant influences on each other. But when $x(I)$ and $z(I)$ get into the ranges where f_1 and f_2 change rapidly, the homeostatic plateau is created. Finally, when I is high, the influences again are constant and $z(I)$ resumes its rapid rise.

6 Multiple Motifs in One Network

We have discussed separately four homeostatic biochemical motifs, but, of course, more than one can occur even in a very simple network. Figure 11 shows a network that contains feedforward excitation, $f_2(x)$, feedback inhibition, $f_1(z)$, and the kinetic motif $g_2(y)$. Each one alone would create homeostasis for z over an interval of I input values, with escape from homeostasis to the right and the left of the interval. What happens if all three are present?

The answer depends on the ranges of x, y,, and z values over which the nonlinear functions f_1, f_2, and g_2 change rapidly. If those regions overlap, the homeostatic

Fig. 11 Three homeostatic mechanisms: feedforward excitation, feedback inhibition, and the kinetic motif in one small network
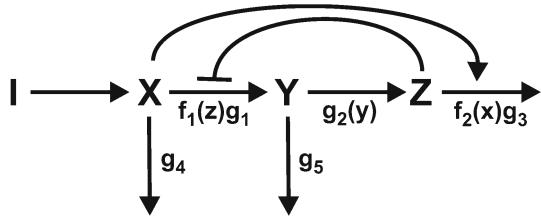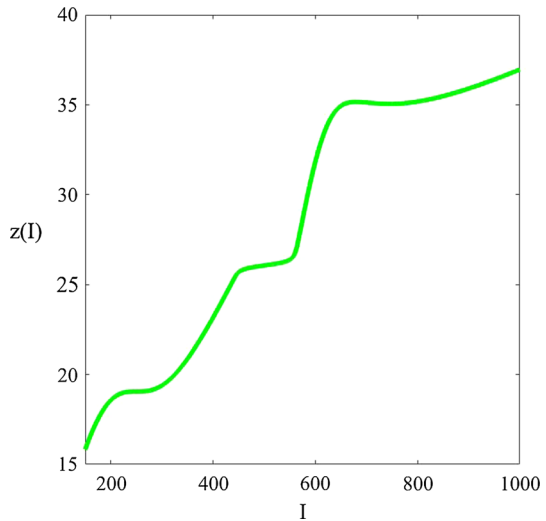

Fig. 12 Three homeostatic plateaus in $z(I)$ for the network in Fig. 11. The differential equations, the functions $f_1(z)$, $g_2(y)$, and $f_2(x)$, and the parameters are similar to those given in Sects. 2, 3 and 4.

effects can be additive, or if they are disjoint, the effects can occur over separate ranges of the input parameter, I. The latter case is illustrated by the simulation in Fig. 12. Feedforward excitation kicks in first for fairly low values of I. Then, for higher values of I, the feedback inhibition motif makes a homeostatic plateau. Finally, for very high values of I, the kinetic motif (from Panel C of Fig. 8) creates a third plateau. To the left and right, we see the expected escape from homeostasis. In the central region, the concentration of z takes on one of three homeostatic levels with fairly rapid transitions between them.

One interesting aspect of the phenomenon in Fig. 12 is that it shows that, even though concentrations vary continuously, a concentration can essentially have three distinct values with rapid transitions between them as I is varied over the middle range. These three distinct values for z are not created by different equilibria but by three different homeostatic mechanisms.

Finally we note that if one adds a second motif to a motif in a network, then one can change the nature of the first motif. In Sect. 5 we showed that the parallel inhibition motif cannot have a GS homeostasis point. However, if one adds a kinetic motif, then the parallel inhibition motif can have a GS homeostasis point.

Theorem 6 *Assume all of the hypotheses of Theorem 5 for the parallel inhibition motif except that we relax the hypothesis on g_3 to allow points where $g_3'(x_0) = 0$. Then, the GS homeostasis points of z are exactly at the equilibria where $g_3'(x_0) = 0$.*

Proof As in the proof of Theorem 5, we let $g_1(I_1) = 1$. Let $(x(I), z(I))$ be a family of equilibria. Differentiation with respect to I yields

$$f_1'(z)z'(I) = g_3'(x)x'(I)$$
$$g_2'(I) = \left[g_5'(z) + \frac{\partial h}{\partial z} \right] z'(I) + \left(\frac{\partial h}{\partial x} \right) x'(I). \qquad (19)$$

Observe that $z'(I_0) = 0$ if and only if

$$g_3'(x_0)x'(I_0) = 0 \quad \text{and} \quad \left(\frac{\partial h}{\partial x} \right) x'(I) = g_2'(I_0).$$

Since $g_2'(I_0) > 0$, it follows that $x'(I_0) \neq 0$ and hence that $g_3'(x_0) = 0$. Conversely, if $g_3'(x_0) = 0$, then the first equation implies $z'(I_0) = 0$ since $f_1'(z_0) < 0$. □

This phenomenon is interesting because the kinetic motif in the catabolism of x creates a GS homeostasis point in a different variable, z, that is neither the substrate nor the product of the kinetic motif itself.

7 Motifs in a Real Biological Network

Motifs of the kind we have been considering occur in large, realistic biological networks. For example, the folate and methionine cycles in liver cells are depicted in Fig. 13, and we shall see that all four of the motifs that we have discussed occur there. The rectangular boxes indicate the substrates and the blue ellipses contain the acronyms of the enzymes that catalyze the reactions. The amino acids serine, glycine, and methionine, are inputs to this part of one-carbon metabolism. For simplicity, we will assume the concentrations of serine and glycine are constant and focus on the effects of changes in methionine input. After meals, amino acid concentrations in the blood increase by a factor of 2–6 Kilberg and Haussinger (1992). How does the cell maintain homeostasis in these cycles with such a large change in methionine input? The answer is with a large set of overlapping homeostatic mechanisms, including the four mechanisms we have singled out in this paper.

When methionine input goes up dramatically, one would expect all the substrates of the methionine cycle, methionine (MET), s-adenosyl-methionine (SAM), s-adenosyl-homocysteine (SAH), and homocysteine (Hcy) to rise accordingly. Since Hcy is the major biomarker for cardiovascular disease Clarke and Banfield (2001), one might expect that the cell has a mechanism to keep the Hcy concentration from rising too high. This mechanism is feedforward excitation from SAM that activates the enzyme CBS that sends Hcy down the transsulfuration pathway. Figure 3 in Nijhout et al. (2014) shows that the steady-state Hcy concentration has a chair shape and is quite homeostatic over a wide range of methionine inputs.
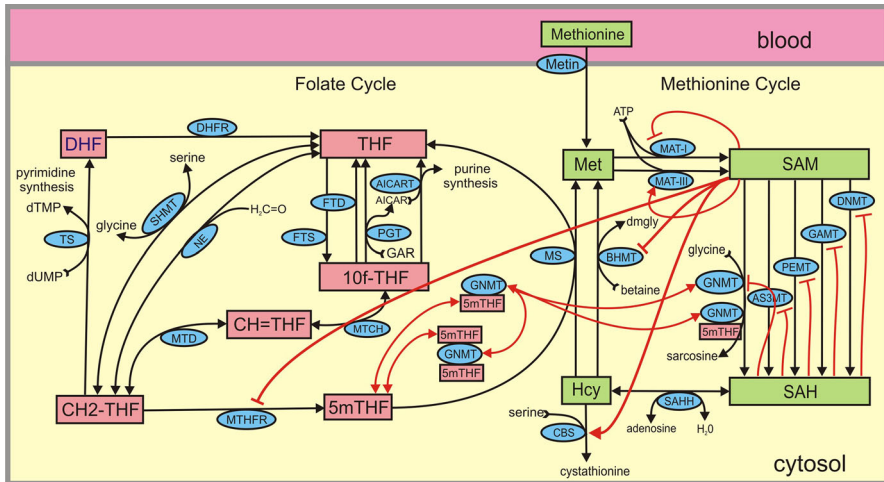
Fig. 13 The folate and methionine cycles. The *green* and *pink boxes* represent substrates and the *blue ellipses* contain the acronyms of the enzymes catalyzing particular reactions. The complete set of differential equations and kinetics formulas for all the reactions, including the *red* homeostatic mechanisms, can be found in Reed et al. (2014) (Color figure online)

The reactions from SAM to SAH on the right side of the diagram are methyltransferase reactions in which a methyl group is taken from SAM and attached to some substrate leaving SAH and the methylated substrate. There are over 150 methyltransferase reactions that use SAM as the substrate; we have depicted five important ones. The DNMT reaction attaches methyl groups to cytosines in promoter regions of genes (the basis of epigenetics). The AS3MT reaction replaces a oxygen bound to arsenic with a methyl group, which helps in detoxifying arsenic. The GAMT reaction is the final step in the synthesis of creatine, and the PEMT reaction is a major step in the construction of cell membranes. Almost all the methyltransferase reactions show strong or weak product inhibition from SAH Clarke and Banfield (2001). In one case, the "purpose" of the production inhibition is clear. When blood methionine goes up, SAM goes up as does the product SAH. The increased SAM drives the PEMT reaction faster, and the increased SAH inhibits the PEMT reaction. These two effects almost exactly cancel, so the PEMT reaction hardly varies as blood methionine changes Reed et al. (2014).

The pink boxes on the left side of the diagram are all different forms of folate, vitamin B-9, which comes from green vegetables. The TS reaction and the AICART reaction are major steps in the synthesis of pyrimidines and purines, respectively, so the folate cycle is highly upregulated when the cell is trying to divide. The enzymes TS and DHFR are the targets of the chemotherapeutic agents 5-fluorouracil and methotrexate that attempt to disrupt this function of the folate cycle. Almost all of the folate substrates bind non-enzymatically and reversibly to various of the folate enzymes, taking both the substrate and the enzyme out of service. This is a kind of substrate inhibition as was discussed in Sect. 4. As the total folate in the liver decreases (because of the lack of vegetables), some of the reversible bonds dissociate making both more folate and

more enzyme available. We have shown that, because of this substrate inhibition, the velocity of the reactions in the folate cycle change very little as the total liver folate varies from normal to 25% of normal and have proposed that this effect protected our ancestors against the lack of vegetables in the winter Nijhout et al. (2004).

The diagram shows that SAM inhibits the enzyme MTHFR in the folate cycle, and the product of that reaction, 5 m THF, inhibits the enzyme GNMT, which is a methyl transferase. This is the parallel inhibition motif. To understand what this regulation does, one needs to understand that the parallel methyltransferase reactions pose a serious problem for the cell: they all have the same substrate, SAM. By upregulating and downregulating the individual methyltransferases, the cell could hope to control the individual fluxes of the reactions. However, suppose one of the reactions, say GAMT, is downregulated to zero (if you eat plenty of creatine, the body doesn't need to synthesize it and GAMT is downregulated). Then SAM will go up, and the other methyltransferase reactions will tend to go faster. Thus, because the methyltransferase reactions all use the same substrate, it is hard for the cell to regulate them individually. The parallel inhibition motif helps the cell to solve this problem. Suppose the GAMT reaction is downregulated. Then SAM will start to go up. This inhibits MTHFR more, so the 5mTHF concentration will drop. This removes some of the inhibition of GNMT so the GNMT reaction will go faster preventing SAM from going up very much. Similarly, if the GAMT reaction goes up, the same chain of reasoning (with "increases" and "decreases" switched) shows that SAM won't change too much. The parallel inhibition motif was discovered by Wagner Wagner et al. (1985) who dubbed GNMT the "salvage pathway." We have shown with mathematical modeling that it actually does work that way, and we have shown that this mechanism is very effective at keeping the DNA methylation reaction going at a constant rate Reed et al. (2014), Nijhout et al. (2006).

Thus all four of the motifs discussed in Sects. 2–5 occur in this pathway. And there is more. Normally, about half the flux that arrives at Hcy from SAH is directed to the transsulfuration pathway via CBS, and half is recirculated to Met via the reactions MS and BHMT. However, as indicated in the diagram, SAM inhibits BHMT. When methionine in the blood goes up after a meal, SAM rises which increases the inhibition of BHMT. This sends more Hcy down the CBS pathway and less back to Met via BHMT, and this tends to stabilize the total mass in the methionine cycle. Finally, notice in the diagram that SAM excites one of the enzymes that synthesizes it (MAT-III) and inhibits the other enzyme that synthesizes it (MAT-I). We are not certain what this regulation is for, but in our computational experiments, it seems to prevent large swings in the Met concentration.

8 Discussion

Biochemical networks (for example, the folate and methionine cycles, Fig. 13) are complicated but traditionally understood as flow diagrams through which one can track influences and changes in concentration. However, many of the regulatory mechanisms that we have discussed involve substrates at one location in the network influencing enzymes that catalyze distant reactions in the network. When one adds these regulatory mechanisms, it is not easy to see how the network will respond to perturbations because

the mechanisms are non-local in the network, and it is not easy to see what the emergent properties of the network are. Homeostasis of some substrate concentrations and some velocities in the face of large changes in amino acid inputs is an important emergent property of all the biochemical networks that we have studied Nijhout et al. (2004), Reed et al. (2008), (2014), Best et al. (2010). Thus the study of how the homeostasis comes about and breaks down is a crucial part of understanding cell metabolism.

In this study, we have analyzed four different mechanisms: feedforward excitation, feedback inhibition, the kinetic motif, and the parallel inhibition motif. All occur in folate and methionine metabolism. Golubitsky and Stewart (2017) proposed that a good way to find homeostatic nodes in a network is to look for nodes z and input values I_0 at which $z'(I_0) = 0$ and $z''(I_0) = 0$. Interestingly, we found that two of our motifs have this property and that although the other two do not, they all show homeostatic plateaus and exhibit escape from homeostasis. So some mechanisms show homeostasis, but they do not have GS singularities.

In our analysis of the motifs, the regulations are given by nonlinear functions of substrate concentration but, except for the the kinetic motif, we have not discussed the actual excitatory and inhibitory mechanisms, which are themselves normally constructed out of biochemical mechanisms. These mechanisms are very diverse. Some metabolites bind to promoter regions of genes and influence the expression of genes that code for enzymes. Some metabolites bind to sites on enzymes and change the conformation of the enzyme and thus its activity. And some metabolites compete directly for the substrate's binding site.

There are several natural and important questions that we have not addressed. First, what determines the height of the homeostatic plateau? This is called the "set point" in physiological systems. For example, what determines body temperature, or salt concentration in the blood, or diastolic blood pressure. These set points can change over short and long times, and understanding how they are set would contribute to medical understanding. In the four simple motifs, one can study how the set point is affected by the parameters and the nonlinear function that represents the regulation. A second natural biomedical question is to determine which parameters and which properties of the nonlinear control function affect the width of the homeostatic plateau. For both questions, new understanding would lead to possible intervention strategies to change the set point or to widen the plateau.

Since the work of Alon (2007), motifs have been an important topic in biology and systems biology. However, there is a deep and natural question that has not often been addressed. Motifs in real biological networks do not exist in isolation but are imbedded in much larger networks. Under what conditions does the imbedded motif operate in the same way as the isolated motif? Of course, the natural answer is, "if the influence of rest of the network on the motif is small and the influence of the motif on the rest of the network is small." A rigorous formulation of this principle seems to require complicated estimates and technical conditions, but it broadly supports that intuition. The results depend on exactly how the motif is coupled into the rest of the network.[1]
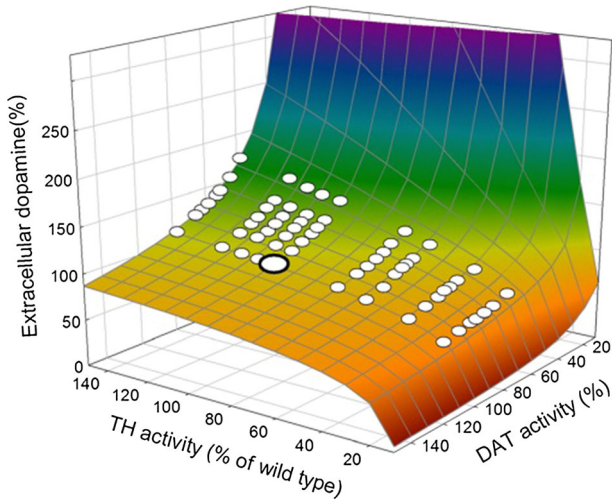
---

[1] Golubitsky and Stewart, in preparation.

Fig. 14 Extracellular dopamine as a function of TH and DAT activity. TH is the rate-limiting enzyme for the synthesis of dopamine and DAT transports dopamine from the extracellular space to the terminal cytosol. These are computations from a mathematical model Best et al. (2009), Nijhout et al. (2014) that includes various regulatory mechanisms for dopamine. "Normal" is represented by the large *white dot* in the homeostatic plateau. The small *white dots* are combinations of polymorphisms in the human population in the genes that code for TH and DAT. They are all on the plateau because if they weren't they would have been selected against (Color figure online)

Finally, we have considered motifs that generate homeostasis in one variable as a function of an input variable. But one is interested also in homeostasis as a function of many variables or parameters and there is no reason why those variables or parameters need to be inputs. Here is an example. Figure 14 shows the dopamine concentration in the extracellular space in the brain as a function of the activity of tyrosine hydroxylase (TH) and the activity of the dopamine transporter (DAT) computed from a mathematical model Best et al. (2009), Nijhout et al. (2014). TH is the rate-limiting enzyme in dopamine neurons in the pathway that synthesizes dopamine. DAT is the transporter that puts dopamine back in the neuron terminal after it has been released in the extracellular space. The large white dot represents "normal," and as one can see, it is in the middle of a large homeostatic plateau. The small white dots are combinations of many of the polymorphisms in TH and DAT in the human population. They are all on the homeostatic plateau! In others words, it does not matter much how well or poorly your TH and DAT function, your dopamine in the extracellular space will remain about the same (because of regulatory mechanisms that we haven't described). So, the natural challenge is to design mathematical methods to find such higher dimensional plateaus in biochemical networks. For example, there is an analog of GS chairs in two input systems; it is the hyperbolic umbilic of elementary catastrophe theory. Figure 14 exhibits the mathematical characteristics of the hyperbolic umbilic; see Golubitsky et al. (2017).

The idea of personalized (or precision) medicine is that there is great biological variation and therefore patient treatments should be designed based on the individual

characteristics of patients. What characteristics? Well, certainly their genotype, but also their diet, their exercise patterns, the air they breathe, and so forth. These last variables are very hard to quantify especially since one would want to know them over the patient's lifetime. But determining a patient's genotype is cheap and easy. So researchers expect that we can determine treatments based on genotype alone. But as the surface in Fig. 14 shows, the genotype may be very different, but the phenotype (the extracellular dopamine concentration) may remain the same because of regulatory biochemical mechanisms. Thus, it unlikely that personalized medicine treatment strategies based on genotype alone will work well.

Author contributions All authors contributed to the ideas in the manuscript. Golubitsky and Stewart did the calculations about GS homeostasis points and GS chairs. MR and JB did the other analytical calculations. MR, JB, and HFN wrote the manuscript. All authors read, edited, and approved the manuscript.

Compliance with Ethical Standards

Conflicts of interest No competing interests declared.

References

Alon Y (2007) An introduction to systems biology: design principles of biological circuits. Chapman and Hall, Boca Raton

Becker A, Schloder P, Steele J, Wegener G (1996) The regulation of trehalose metabolism in insects. Experientia 52:433–439

Benoit-Marand M, Borelli E, Gonon F (2001) Inhibition of dopamine release via presynaptic D2 receptors. Neuroscience 21(9):34–41

Best J, Nijhout MRHF (2009) Homeostatic mechanisms in dopamine synthesis and release: a mathematical model. Theor Biol Med Model 6(1):21

Best J, Nijhout MRHF (2010) Serotonin synthesis, release, and reuptake in terminals: a mathematical model. Theor Biol Med Model 7(1):34

Cannon WB (1926) A Charles Richet : ses amis, ses collègues, ses élèves, Paris: Les Éditions Médicales 1926 chap. Physiological regulation of normal states: some tentative postulates concerning biological homeostatics

Chaplin M, Burke C (1990) Enzyme technology. Cambridge University Press, Cambridge

Clarke S, Banfield K (2001) S-adenosyl-methionine dependent methyltransferases. Homocysteine in health and disease. Cambridge University Press, Cambridge, pp 63–78

Cornish-Bowden A (2012) Fundamentals of enzyme kinetics. Portland Press, Portland

Drengstig T, Jolma I, Ni X, Thorsen K, Xu X, Ruoff P (2012) A basic set of homeostatic controller motifs. Biophys J 103:2000–2010

Elliott D, Newman K, Forward D, Hahn D, Ollivere B, Kojima K, Handley R, Rossiter N, Wixted J, Smith R, Moran C (2016) A unified theory of bone healing. Bone and Joint J 98–B:884–91

Golubitsky M, Stewart I (2017) Homeostasis, singularities and networks. J Math Biol 74(1–2):387–407. doi:10.1007/s00285-016-1024-2

Golubitsky M, Stewart I, Best J, Reed M, Nijhout F (2017) Homeostasis with multiple inputs. Preprint

Green N, Lee L (2012) Modern and evolving understanding of cerebral perfusion and autoregulation. Adv Anesth 30:97–129

Haldane J (1930) Enzymes. Longmans, Green, and Co, New York

Hall J (2017) Guyton and Hall textbook of medical physiology, 13th edn. Elsevier, Philadelphia

Kilberg M, Haussinger D (eds) (1992) Mammalian amino acid transport; mechanisms and control. Plenum Press, New York

Michaelis L, Menten M (1915) Die kinetic der invertinwirkung. Biochem Z 49:333–369

Nijhout HF, Reed M (2014) Homeostasis and dynamic stability of the phenotype link robustness and stability. Int Comp Biol 54:264–275

Nijhout HF, Reed M, Budu P, Ulrich C (2004) A mathematical model of the folate cycle: new insights into folate homeostasis. J Biol Chem 226:33–43

Nijhout HF, Reed M, Anderson D, Mattingly J, James SJ, Ulrich C (2006) Long-range allosteric interactions between the folate and methionine cycles stabilize the DNA methylation reaction. Epigenetics 1:81–87

Nijhout HF, Best J, Reed M (2014) Escape from homeostasis. Math Biosci 257:104–110

Nijhout HF, Best J, Reed M (2015) Using mathematical models to understand metabolism, genes and disease. BMC Biol 13(1):79

Reed M, Thomas R, Pavisic J, James SJ, Ulrich C (2008) A mathematical model of glutathione metabolism. Theor Biol Med Model 5(1):8

Reed M, Lieb A, Nijhout HF (2010) The biological significance of substrate inhibition: a mechanism with many functions. BioEssays 32:422–429

Reed M, Gamble M, Hall M, Nijhout HF (2014) Mathematical analysis of the regulation of competing methyltransferases. BMC Syst Biol 9(1):69

Segel IH (1975) Enzyme kinetics. Wiley-Interscience, New York

Segel L (1984) Modeling dynamic phenomena in molecular and cellular biology. Cambridge University Press, Cambridge

Storey K (ed) (2004) Functional metabolism: regulation and adaptation. Wiley-Liss, Hoboken

Segel L (ed) (1980) Mathematical models in molecular and cellular biology. Cambridge University Press, Cambridge

Wagner C, Briggs WT, Cook RJ (1985) Inhibition of glycine N-methyltransferase activity by folate derivatives: implications for regulation of methyl group metabolism. Biochem Biophys Res Commun 127:746–752